Supporting Information

Enhanced photocatalytic degradation of organic pollutants and hydrogen production by a visible light–responsive $Bi_2WO_6/ZnIn_2S_4$ heterojunction

Auttaphon Chachvalvutikul[a], Tawanwit Luangwanta[a], Samuel Pattisson[b], Graham J. Hutchings[b], Sulawan Kaowphong[a,c,d,*]

[a] Department of Chemistry, Faculty of Science, Chiang Mai University, Chiang Mai 50200, Thailand

[b] Cardiff Catalysis Institute, School of Chemistry, Cardiff University, Main Building, Park Place CF10 3AT, Cardiff, UK

[c] Center of Excellence in Materials Science and Technology, Chiang Mai University, Chiang Mai 50200, Thailand

[d] Center of Excellence for Innovation in Chemistry, Faculty of Science, Chiang Mai University, Chiang Mai 50200, Thailand

*Corresponding author

E–mail address: sulawank@gmail.com, sulawan.k@cmu.ac.th

Tel: +66 53 943341 Fax: +66 53 892277

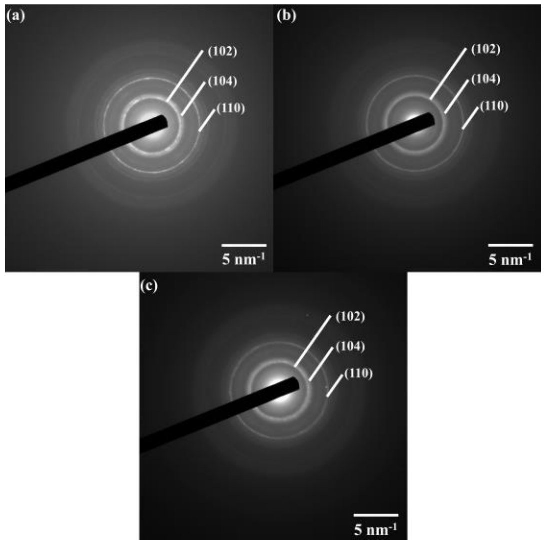

Fig. S1. SAED patterns of the $ZnIn_2S_4$ samples synthesized using **(a)** 30, **(b)** 45 and **(c)** 60 cycles of microwave irradiation.

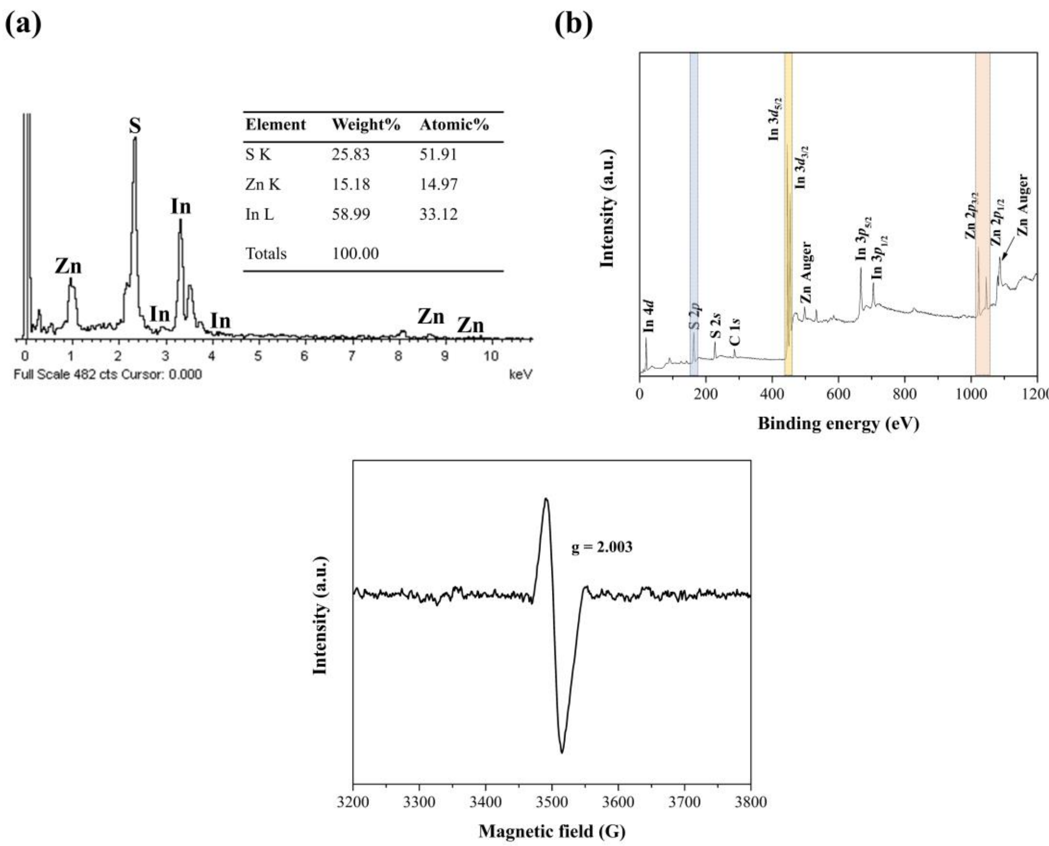

Fig. S2. **(a)** EDS, **(b)** survey XPS and **(c)** EPR spectra of the synthesized $ZnIn_2S_4$ material.

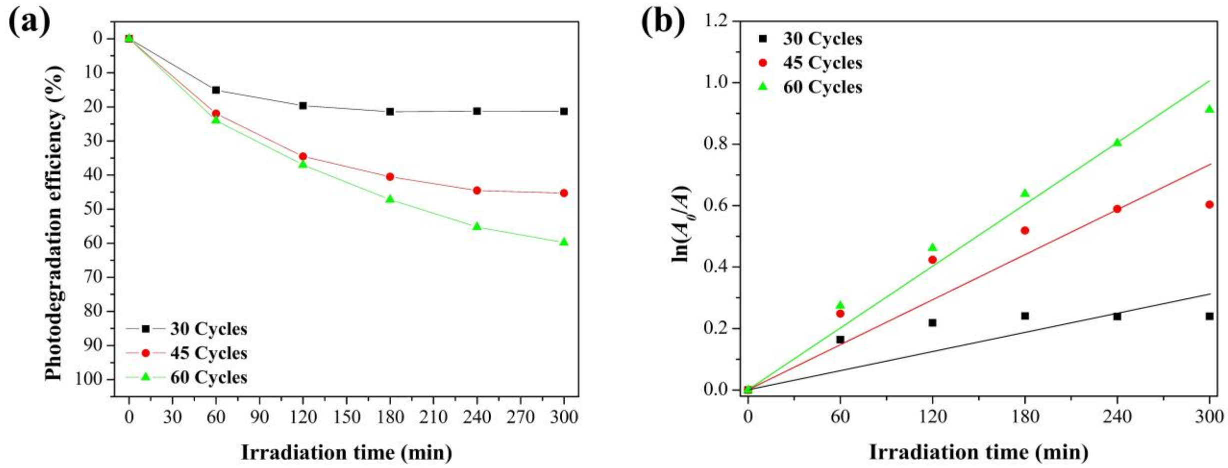

Fig. S3. (a) Photodegradation efficiency of the $ZnIn_2S_4$ photocatalyst samples towards MB and **(b)** the corresponding kinetic plots.

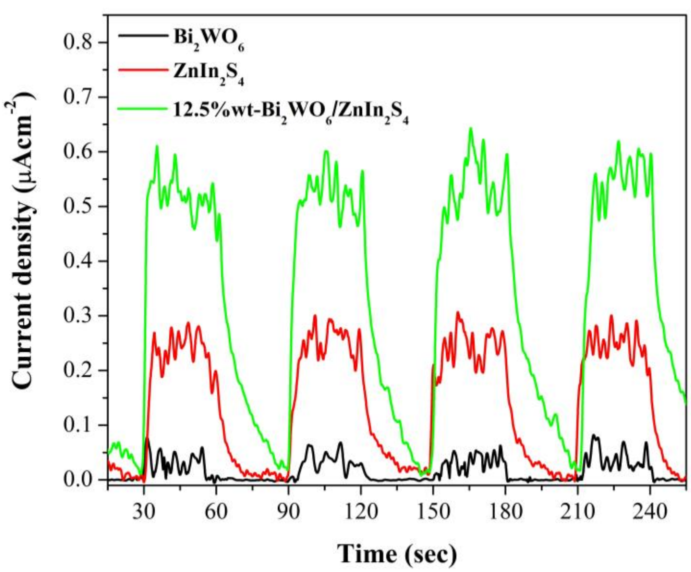

Fig. S4. Transient photocurrent response of Bi_2WO_6, $ZnIn_2S_4$ and 12.5%wt-Bi_2WO_6/$ZnIn_2S_4$.

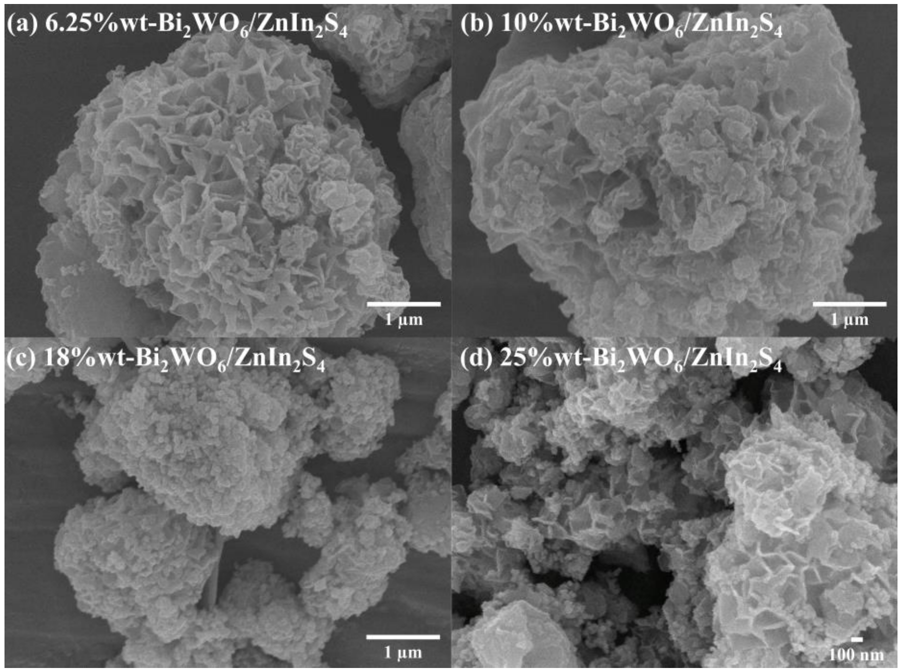

Fig. S5. FESEM images of the $Bi_2WO_6/ZnIn_2S_4$ nanocomposites with **(a)** 6.25, **(b)** 10, **(c)** 18 and **(d)** 25 %wt of Bi_2WO_6, respectively.

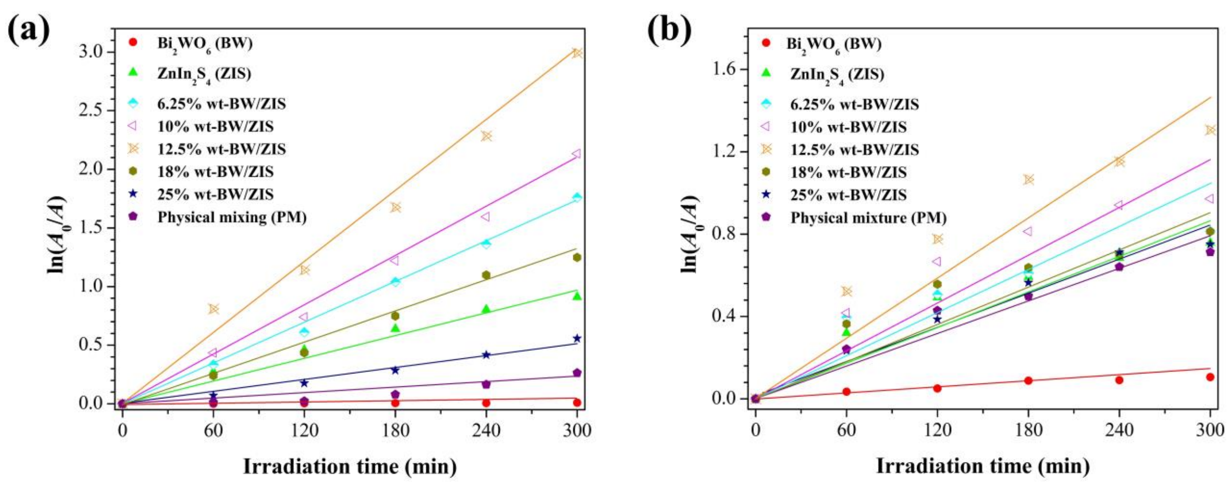

Fig. S6. Kinetic plots of the photocatalytic degradations of **(a)** MB and **(b)** SA.

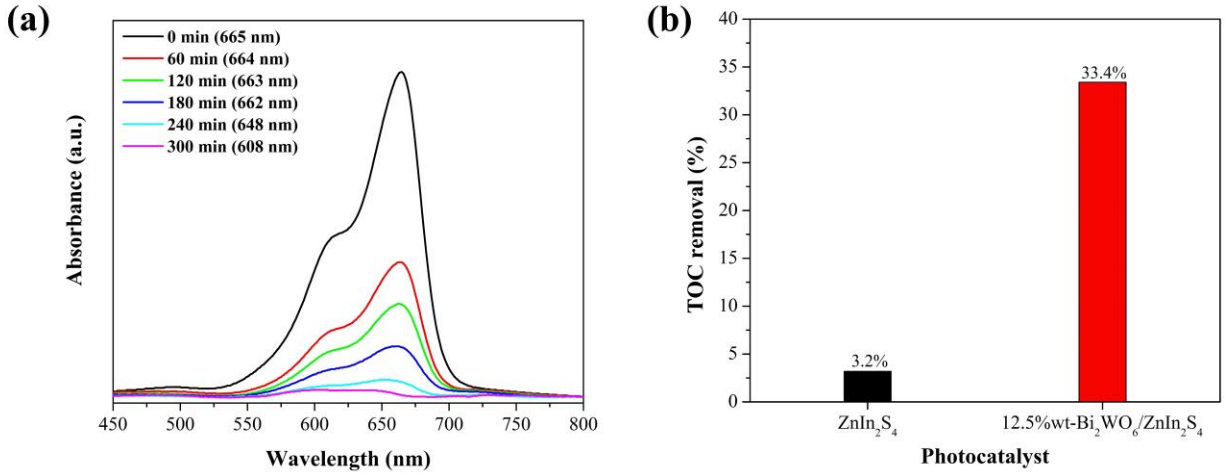

Fig. S7. (a) The changes in the absorption spectra during the photodegradation process of the MB in the presence of the 12.5%wt-$Bi_2WO_6/ZnIn_2S_4$ photocatalyst and **(b)** TOC removal of MB over 12.5%wt-$Bi_2WO_6/ZnIn_2S_4$ and $ZnIn_2S_4$ under 300 min of visible-light irradiation.

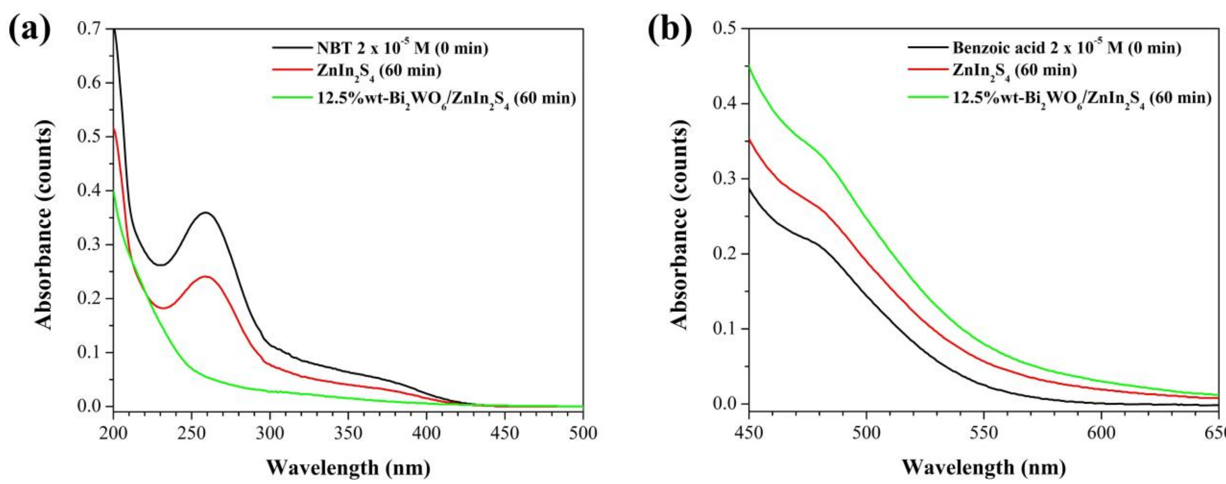

Fig. S8. The detection of $O_2^{\bullet-}$ and $^{\bullet}OH$ radicals using nitrotetrazolium blue (NBT) transformation and benzoic acid hydroxylation methods, respectively. The absorption spectra of **(a)** nitrotetrazolium blue and **(b)** Fe(III)-hydroxybenzoic acid complex supernatant solutions.

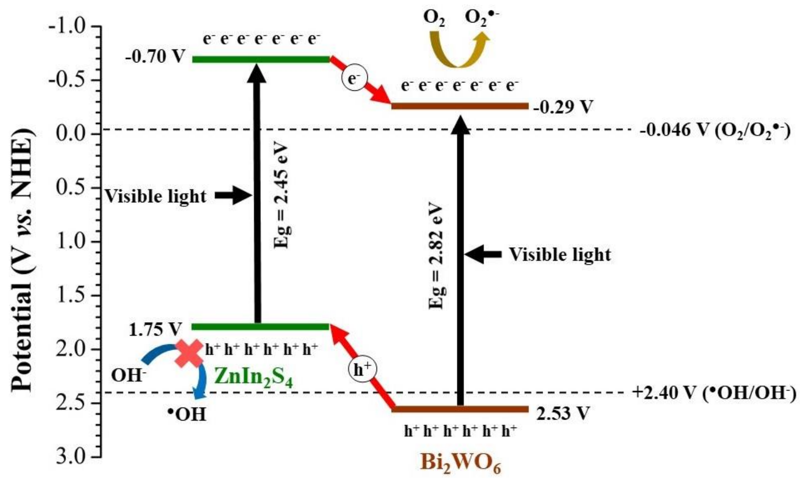

Fig. S9. A conventional charge transfer mechanism of 12.5%wt-Bi_2WO_6/$ZnIn_2S_4$ heterojunction.

Table S1. Photodegradation efficiency (%DE), calculated initial rate constants (k, min^{-1}) and the corresponding coefficient of determination (R^2) of the photocatalysts toward SA and MB photodegradation.

Photocatalysts	Methylene blue			Salicylic acid		
	%DE	***k* (min^{-1})**	**R^2**	**%DE**	***k* (min^{-1})**	**R^2**
Bi_2WO_6	0.97	0.00003	0.9831	14.0	0.0006	0.9809
$ZnIn_2S_4$	59.8	0.0033	0.9916	53.2	0.0029	0.9656
6.25%wt-Bi_2WO_6/$ZnIn_2S_4$	82.8	0.0057	0.9988	55.7	0.0031	0.9592
10%wt-Bi_2WO_6/$ZnIn_2S_4$	88.2	0.0069	0.9983	62.1	0.0039	0.9599
12.5%wt-Bi_2WO_6/$ZnIn_2S_4$	95.0	0.0098	0.9966	72.9	0.0050	0.9707
18%wt-Bi_2WO_6/$ZnIn_2S_4$	71.3	0.0042	0.9964	55.6	0.0031	0.9562
25%wt-Bi_2WO_6/$ZnIn_2S_4$	42.7	0.0017	0.9927	52.8	0.0028	0.9875
Physical mixture (PM)	23.1	0.0007	0.9970	51.0	0.0026	0.9812